From a Natural Product Lead to the Identification of Potent and Selective Benzofuran-3-yl-(indol-3-yl)maleimides as Glycogen Synthase Kinase 3β Inhibitors That Suppress Proliferation and Survival of Pancreatic Cancer Cells

Irina N. Gaisina,[†] Franck Gallier,[†] Andrei V. Ougolkov,[‡] Ki H. Kim,[†] Toru Kurome,[†] Songpo Guo,[†] Denise Holzle,[§] Doris N. Luchini,[‡] Sylvie Y. Blond,[§] Daniel D. Billadeau,*,[‡] and Alan P. Kozikowski*,[†]

Drug Discovery Program, College of Pharmacy, Department of Medicinal Chemistry and Pharmacognosy, University of Illinois at Chicago, 833 South Wood Street, Chicago, Illinois 60612, Department of Medicinal Chemistry and Pharmacognosy and the Center for Pharmaceutical Biotechnology, University of Illinois at Chicago, 900 South Ashland, Chicago, Illinois 60607, and College of Medicine, Department of Immunology and Division of Oncology Research, Mayo Clinic, 13-42 Guggenheim, 200 First Street SW, Rochester, Minnesota 55905

Recent studies have demonstrated that glycogen synthase kinase 3β (GSK-3β) is overexpressed in human colon and pancreatic carcinomas, contributing to cancer cell proliferation and survival. Here, we report the design, synthesis, and biological evaluation of benzofuran-3-yl-(indol-3-yl)maleimides, potent GSK-3β inhibitors. Some of these compounds show picomolar inhibitory activity toward GSK-3β and an enhanced selectivity against cyclin-dependent kinase 2 (CDK-2). Selected GSK-3β inhibitors were tested in the pancreatic cancer cell lines MiaPaCa-2, BXPC-3, and HupT3. We determined that some of these compounds, namely compounds **5**, **6**, **11**, **20**, and **26**, demonstrate antiproliferative activity against some or all of the pancreatic cancer cells at low micromolar to nanomolar concentrations. We found that the treatment of pancreatic cancer cells with GSK-3β inhibitors **5** and **26** resulted in suppression of GSK-3β activity and a distinct decrease of the X-linked inhibitor of apoptosis (XIAP) expression, leading to significant apoptosis. The present data suggest a possible role for GSK-3β inhibitors in cancer therapy, in addition to their more prominent applications in CNS disorders.

Introduction

Glycogen synthase kinase 3 (GSK-3[a]) was identified in the late 1970s and originally found to regulate glycogen metabolism.[1] Later, this enzyme has attracted immense interest due to its diverse roles in cellular events. It is well established that GSK-3 affects a variety of biological processes such as cell cycle progression, proliferation, apoptosis, signaling, and transcription by phosphorylation of many different substrates. In mammals, GSK-3 consists of two distinct isoforms, α and β,[2] which are highly homologous within their ATP binding domain, whereas they are significantly different in their terminal regions. This serine/threonine kinase is constitutively active in resting cells and physiologically inhibited by distinct signaling pathways at multiple levels in stimulated cells. GSK-3β is negatively regulated, for example, by post-translational phosphorylation of Ser-9 located in the N-terminal domain.[3] GSK-3β is also phosphorylated constitutively at Tyr-216; this phosphorylation step appears to take place through autophosphorylation and plays a role in stabilizing the enzyme. In addition, there are different extracellular stimuli and proteins that can regulate this enzyme. For example, GSK-3β is inhibited by the presence of secreted glycoproteins, the so-called Wnts, that function in a pathway that is crucial for the determination of the cell's fate during embryonic development.[4] The Wnt signaling targets a particular subcellular pool of GSK-3β, in which it is complexed to axin, β-catenin, and the adenomatous polyposis coli (APC) proteins. This protein complex is disrupted during Wnt signaling as a result of the displacement of axin by other proteins, such as disheveled and FRAT (frequently rearranged during advanced T-cell lymphomas, also called GBP (GSK-3-binding protein)) proteins. The resulting dephosphorylation of β-catenin leads to its accumulation and translocation to the nucleus, where it forms a transcriptional complex with Tcf and Lef family proteins subsequently stimulating activation of several oncogenes. In earlier publications, it was indicated that GSK-3β plays the role of tumor suppressor by down-regulating various proto-oncoproteins.[5−7] Consequently, GSK-3β inhibitors have been considered to possibly mimic the Wnt signaling pathway and to be potentially oncogenic.[3] However, in spite of these concerns, it is well-known that long-term use of lithium, a nonspecific GSK-3β inhibitor, for the treatment of bipolar disorder is not associated with an increased risk of cancer.[8] Moreover, lithium actually increases the survival rates of patients with adenocarcinomas.[9] The administration of the GSK-3β inhibitor 6-{2-[4-(2,4-dichlorophenyl)-5-(4-methyl-1*H*-imidazol-2-yl)pyrimidin-2-ylamino]ethylamino}nicotinonitrile (CHIR 99021)[10] in Zucker diabetic fatty (ZDF) rats for up to 20 h was found not to cause an observable increase in β-catenin or cyclin D1 mRNA in brain, liver, lung, adipose tissue, or colon. Thus, it is possible that the

* To whom correspondence should be addressed. A.P.K.: phone, +1 312 9967577; fax, +1 312 9967107; e-mail, kozikowa@uic.edu. D.D.B.: phone, +1 507 2664334; fax, +1 507 2665146; e-mail, Billadeau.Daniel@mayo.edu.

† Drug Discovery Program, College of Pharmacy, Department of Medicinal Chemistry and Pharmacognosy, University of Illinois at Chicago.

‡ Mayo Clinic.

§ Department of Medicinal Chemistry and Pharmacognosy and the Center for Pharmaceutical Biotechnology, University of Illinois at Chicago, 900 South Ashland, Chicago, IL 60612.

[a] Abbreviations: APC, adenomatous polyposis coli; CDK-2, cyclin-dependent kinase 2; CDKs, cyclin-dependent kinases; DMF-DMA, *N,N*-dimethylformamide dimethyl acetal; DMF-DIPA, *N,N*-dimethylformamide diisopropyl acetal; FRAT, frequently rearranged in advanced T-cell lymphoma; GBP, GSK-3-binding protein; GS, glycogen synthase; GSK-3, glycogen synthase kinase 3; GSK-3β, glycogen synthase kinase 3 isoform type β; NFκB, nuclear factor kappa B; pGS, phosphorylated glycogen synthase; P-gp, permeability-glycoprotein; PKC, protein kinase C; TPSA, total polar surface area; XIAP, X-linked inhibitor of apoptosis; ZDF rat, Zucker diabetic fatty rat.

inhibition of GSK-3β by itself may be unable to elevate β-catenin levels in primary cells; such elevations may require that the cell lines have already undergone some prior transforming events such as APC protein truncation.[11] Recently, a line of evidence led to an indication that GSK-3β is pathologically active in different types of gastrointestinal cancer.[12,13] It was shown that this enzyme is overexpressed in colon and pancreatic cancer cells where it has been implicated in NFκB (nuclear factor kappa B) activation.[14,15] In fact, GSK-3β is found to accumulate in the nucleus of cancer cells and has recently been shown to regulate chromatin structure and the binding of NFκB to its target gene promoters in chronic lymphocytic leukemia cells.[16] Importantly, inhibition of GSK-3β activity in several cancer cell types results in diminished NFκB transcriptional activity of antiapoptotic genes, resulting in apoptosis.[15,16] Thus, GSK-3β has emerged as a promising target in development of new drugs for the treatment of chronic and progressive diseases.[3,17] Over the past decades, a number of small molecule GSK-3 inhibitors have been designed from natural products or known kinase inhibitors[17] for diabetes and neurodegenerative disorders, but only a few of these were tested in cancer cell lines. In the present work we have directed our attention to the possibility to use inhibitors of GSK-3β in the treatment of pancreatic cancer. Our work in this area was influenced by the maleimide-bearing natural product staurosporine, first identified as a protein kinase C (PKC) inhibitor, although it is now known to be able to target other protein kinases, including GSK-3β. From our original screening studies of staurosporine and its analogs, we were led to the design of benzofuran-3-yl-(indol-3-yl)maleimides as GSK-3β inhibitors.[18] In continuation of this work and to gain better insights into the SAR of this benzofuran containing scaffold, a small library of substituted maleimides has been generated. Using structure-based design methods, we have optimized our lead compounds so as to arrive at subnanomolar potency GSK-3β inhibitors that are relatively selective for GSK-3β versus homologous kinases.

Results and Discussion

Chemical Synthesis. The synthesis of the benzofuran-3-yl(indol-3-yl)maleimides (**1**–**38**) (Table 1) is straightforward and based on the condensation of the appropriately substituted 3-indolylglyoxylic acid esters and benzofuranyl-3-acetamides. The general method is shown in Scheme 1 and follows our previously published work.[18] Preparation of indolyl-based glyoxalates commences with *N*-alkylation of the indole **39** followed by acylation of the resulting indole **40** with ethyl oxalyl chloride to afford the precursor **41**. The required benzofuranyl-3-acetamides **44** were prepared from the appropriately substituted 3-benzofuranones **42**. A Horner–Emmons reaction of **42** with (carbethoxymethylene)triphenylphosphorane afforded ethyl (1-benzofuran-3-yl)acetates **43**, which were subsequently converted into the acetamides **44**. Condensation of the acetamides **44** with the glyoxilic esters resulted in formation of the maleimide core.

As we have already synthesized a small set of compounds substituted in the 5-position,[18] it was important to explore the extent to which the introduction of different functionalities, including H-bond donor and acceptor groups to the 6- or 7-position of the indole or benzofuran ring, could be used to adjust kinase selectivity and potency. Based upon the above considerations, we investigated the effects of adding a hydroxy, alkoxy, hydroxymethyl, methoxymethyl, and carboxylic acid group. Accordingly, commercially available 6-hydroxybenzofuran-3-one **45** was protected as its silyl ether **46** (Scheme 2). Treatment of **46** with (carbethoxymethylene)triphenylphosphorane

and subsequent amidation of the intermediate ester provided the acetamide **47**. The alcohol functionality was protected as its *tert*-butyldiphenylsilyl ether (compound **48**) or alkylated with different alkyl and aryl halides (compounds **49**–**54**). Finally, condensation with the appropriate indolylglyoxylic acid esters followed by deprotection of the silyl ether if needed gave a variety of 6-hydroxy substituted maleimides (**4**, **9**, **10**, **16**–**18**) as shown in Table 1.
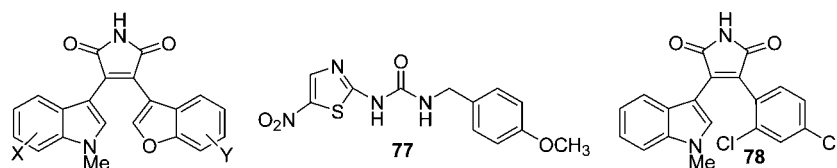
For the introduction of hydroxymethyl and methoxymethyl functionality at the 6-position of the benzofuran moiety, the 3-methoxybenzyl alcohol **55** was converted into the acetate **56** (Scheme 3). Chloroacetylation of **56** and subsequent cyclization of the corresponding aryl ketone **57** yielded the 6-substituted 3-benzofuranone **58**. The general procedure was followed to obtain the 6-hydroxymethylbenzofuranyl-3-acetamide **59**. The acetamide **59** was converted in turn to the methyl ether **60** or silyl ether **61** and then to the maleimides **2**, **3**, **7**, **15**, **23**, **32**, and **34** (Table 1).

Next, our effort was directed to the introduction of a hydroxymethyl, methoxymethyl, or carboxylic acid group at the 7-position of the indole moiety (Scheme 4). Accordingly, the (1*H*-indol-7-yl)methanol **62** was used to synthesize glyoxalates **63** and **64**. The general procedure to form the maleimide was followed to obtain the desired compounds **31** and **33**. The oxidation of the alcohol **33** led to the corresponding aldehyde **65**, which was then subjected to a Horner–Emmons reaction to give the ester **66** (Scheme 5). Treatment with nickel boride, which was generated in situ, resulted in the selective reduction of the double bond and formation of the ester **35**. The latter was converted into the acid **36** by the treatment with sodium hydroxide.

The SAR work was further extended by exploring the effect of polysubstitution of the aromatic rings. Disubstituted indoles were prepared from the corresponding dihalogenated nitrotoluenes **67** and **68** by using a known protocol (Scheme 5).[19] The reaction of **67** and **68** with *N*,*N*-dimethylformamide dimethyl acetal (DMF-DMA) afforded a mixture of the enamine **69** with the methoxy-substituted side-product **70**. In this step, nucleophilic aromatic substitution can be avoided by replacement of DMF-DMA with *N*,*N*-dimethylformamide diisopropyl acetal (DMF-DIPA).[20] A reductive cyclization provided the indoles **71** and **72**.[21] A variety of acetamides prepared from commercially available or made in-house benzofuranones were used in a coupling reaction with oxalates **73**–**76** to prepare the maleimides **5**–**11**. To attach an aromatic ring to the indole, a Suzuki coupling reaction of the appropriate precursor, such as 5-fluoro-6-iodoindole (**5**), with *p*-chlorophenyl boronic acid was employed to afford the final maleimide **12**. In addition, 5,7-dibromo, 5,6-methylenedioxy, and 1*H*-benzo[*g*]indole were used to synthesize compounds **20**, **26**, and **38**, respectively.

Evaluation of the Maleimides to in Vitro Inhibit GSK-3β. The new benzofuran-3-yl-(indol-3-yl)maleimides were screened for their potency to inhibit GSK-3β. Commercially available human GSK-3β was assayed for its ability to phosphorylate the primed peptide substrate (RRRPAS-VPPSPSLSRHSS(P)HQRR; 10 μM) in the presence of 0–30 μM of the maleimides. For comparison purposes, we also determined the IC$_{50}$ values of the known GSK-3β inhibitors **77** (AR-A014418)[22] and **78** (SB-216763)[23] in the same assay. As presented in Table 1, the IC$_{50}$ values vary from poor to excellent (less than 1 nM).

Many GSK-3β inhibitors are also quite potent toward CDK-2 since the ATP binding pockets of these two kinases are very similar.[24] To measure the selectivity of new maleimides, several compounds with different structural features were tested against

Table 1. GSK-3β Inhibition by Substituted Benzofuran-3-yl-(indol-3-yl)maleimides and Compounds **77** and **78**

compd	X	Y	IC$_{50}$^{a} (nM)
77			41.8 ± 6.4
78			50.0 ± 0.2
1^b	H	H	35 ± 9
2	5-F	6-CH$_2$OH	0.35 ± 0.06
3	5-F	6-CH$_2$OCH$_3$	23.8 ± 1.7
4	5-F	6-OH	3.5 ± 1.3
5	5-F, 6-I	7-OCH$_3$	247 ± 28
6	5-F, 6-Cl	H	184 ± 32
7	5-F, 6-Cl	6-CH$_2$OH	0.95 ± 0.19
8	5-F, 6-Cl	6-OCH$_3$	870 ± 160
9	5-F, 6-Cl-	6-cyclopropylmethoxy	1290 ± 360
10	5-F, 6-Cl-	6-cyclobutylmethoxy	4090 ± 820
11	5-F, 6-Cl	7-OCH$_3$	260 ± 32
12	5-F, 6-*p*-Cl-Ph	7-OCH$_3$	7160 ± 1190
13^b	5-Br	H	7.0 ± 3.0
14	5-Br	7-OCH$_3$	7.5 ± 1.1
15	5-Br	6-CH$_2$OH	0.51 ± 0.05
16	5-Br	6-prop-2-ynyloxy	25.3 ± 2.4
17	5-Br	6-allyloxy	48.3 ± 7.0
18	5-Br	6-*O*-(*p*-CH$_3$O)-Bn	335 ± 37
19^b	5-Cl	5-F	42 ± 8
20	5,7-dibromo	7-OCH$_3$	88.7 ± 5.6
21	5-I	H	34.5 ± 3.8
22	5-I	5-F	180 ± 11
23	5-CN	6-CH$_2$OH	13.2 ± 3.2
24^b	5-cyclopropyl	H	235 ± 15
25	5-cyclopropylethynyl	5-F	16.1 ± 3.9
26	5,6-methylenedioxy	5-F	710 ± 160
27	5-OCH$_3$, 6-Cl	H	440 ± 22
28	5-OCH$_3$, 6-I	H	223 ± 22
29^b	6-OH	H	15 ± 3
30	6-CF$_3$	7-OCH$_3$	830 ± 77
31	7-CH$_2$OH	H	5.4 ± 0.7
32	7-CH$_2$OH	6-CH$_2$OH	5.1 ± 1.2
33	7-CH$_2$OMe	H	0.23 ± 0.04
34	7-CH$_2$OMe	6-CH$_2$OH	0.73 ± 0.10
35	7-CH$_2$CH$_2$COOEt	H	10.2 ± 3.6
36	7-CH$_2$CH$_2$COOH	H	1.2 ± 0.2
37^b	7-OH	H	55 ± 8
38	1*H*-benzo[*g*]	5,6-difluoro	314 ± 19

^{a} The ability of commercially available GSK-3β (21 nM, EMD Biosciences, Madison, WI) to phosphorylate the pGS peptide substrate (RRRPAS-VPPSPSLSRHSS(P)HQRR) (10 μM final concentration) was assayed in the presence of 10 μM of ATP (specific activity 1.3 μCi of [γ-^{32}P]ATP/nmol). ^{b} Published in ref 18.

Scheme 1^a
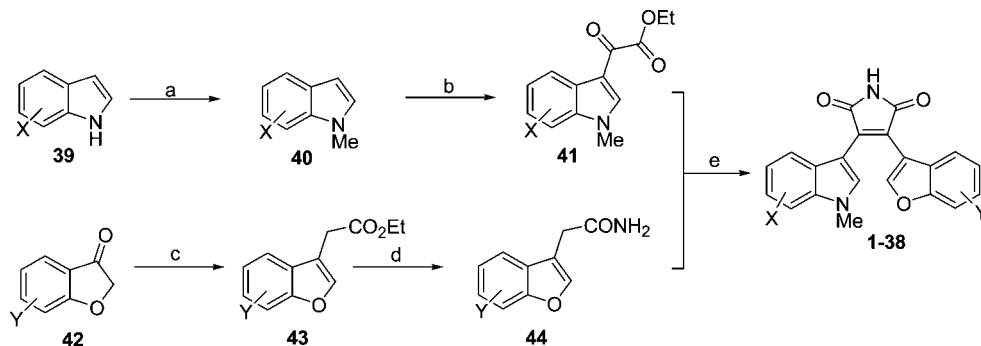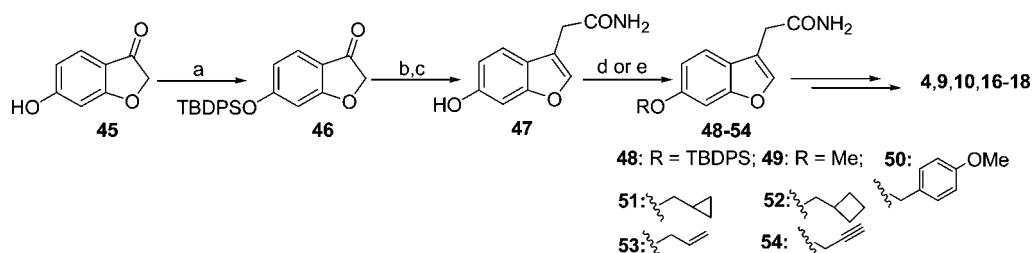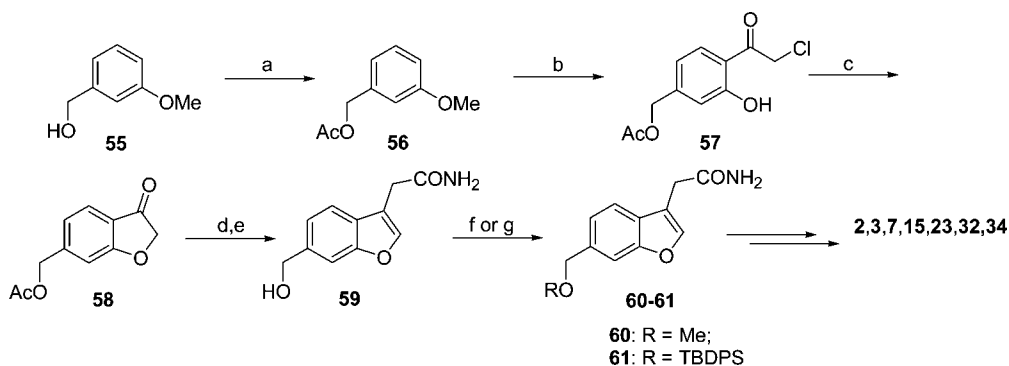

^{a} Reagents and conditions: (a) MeI, NaH, DMF; (b) EtO$_2$CCOCl, Et$_2$O; (c) Ph$_3$P=CH$_2$CO$_2$Et, toluene, 110 °C; (d) NH$_3$/MeOH; (e) *t*-BuOK, THF.

CDK-2/CyclinE. The compounds **2**, **7**, **15**, and **33** were found to be selective toward GSK-3β, based on the ratios of IC$_{50}$ values found for these two kinases (Table 2). From this set, compounds **7**, **11**, **15**, and **33** were selected for more extensive evaluation against a panel of CDKs, and these exhibited a significant level of selectivity (Table 1 in the Supporting Information).

Scheme 2[a]

48: R = TBDPS; **49**: R = Me; **50**: [structure] OMe

51: [structure] **52**: [structure]

53: [structure] **54**: [structure]

[a] Reagents and conditions: (a) TBDPSCl, imidazole, DMF−CH$_2$Cl$_2$; (b) Ph$_3$P=CH$_2$CO$_2$Et, toluene, 110 °C; (c) NH$_3$/MeOH; (d) TBDPSCl, imidazole, DMF−CH$_2$Cl$_2$; (e) CeCO$_3$, Na$_2$CO$_3$, RHal, DMF, 55 °C.

Scheme 3[a]

60: R = Me;
61: R = TBDPS

[a] Reagents and conditions: (a) Ac$_2$O, Et$_3$N, DMAP, CH$_2$Cl$_2$; (b) ClCH$_2$COCl, AlCl$_3$, CH$_2$Cl$_2$, reflux; (c) NaOAc, MeOH; (d) Ph$_3$P=CH$_2$CO$_2$Et, toluene, 110 °C; (e) NH$_3$/MeOH; (f) NaH, MeI, THF, 20 °C; (g) TBDPSCl, imidazole, DMF−CH$_2$Cl$_2$.

Scheme 4[a]

63: R = Me
64: R = TBDPS

31: R = Me
33: R = H
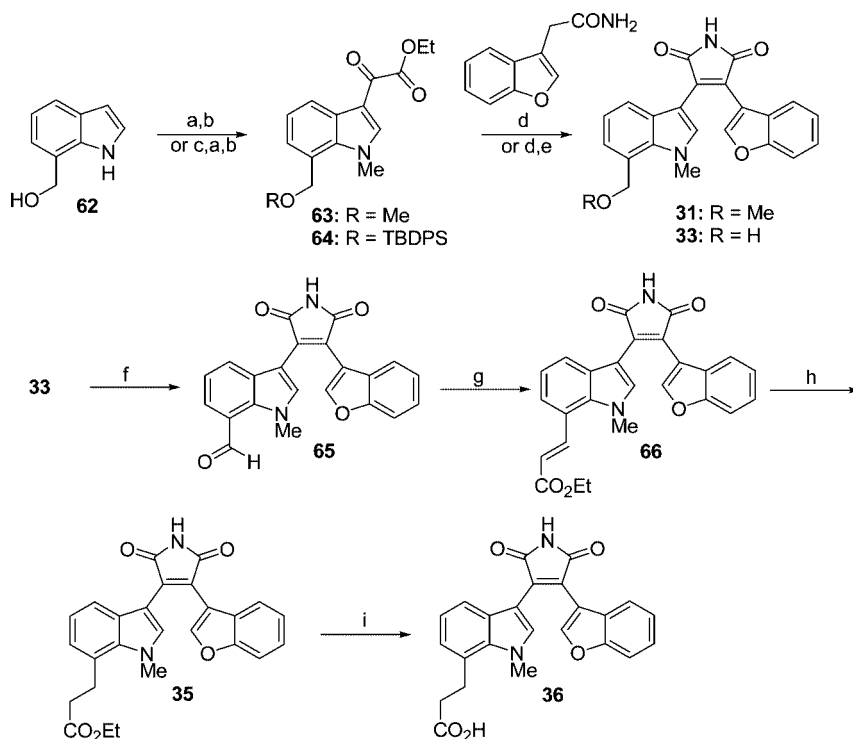
[a] Reagents and conditions: (a) MeI, NaH, DMF; (b) EtO$_2$CCOCl, Et$_2$O; (c) TBDPSCl, imidazole, DMF−CH$_2$Cl$_2$; (d) *t*-BuOK, THF; (e) TBAF, THF; (f) PDC, THF; (g) Ph$_3$P=CH$_2$CO$_2$Et, THF, reflux; (h) NiCl$_2$·6H$_2$O, NaBH$_4$, THF−MeOH; (i) 1 M NaOH, EtOH.

SAR Analysis and Molecular Modeling Studies. Our SAR studies revealed that the introduction of hydrophilic substituents at position 6 or 7 of the indole part of this scaffold is favorable. Indeed, compounds **29** and **31**−**36** demonstrated very good GSK-3β inhibitory activity in an in vitro assay. Compound **33**, bearing a methoxymethyl group, was found to be the best

inhibitor with an IC$_{50}$ = 0.23 ± 0.04 nM. Previously, we discovered that the presence of a halogen in the 5-position of the indole is favorable.[18] This finding was confirmed by the remarkably high activities of compounds **2**−**4** and **13**−**15**. On the other hand, the introduction of an additional halogen led to a reduction in the inhibitory activity of the corresponding

Scheme 5[a]
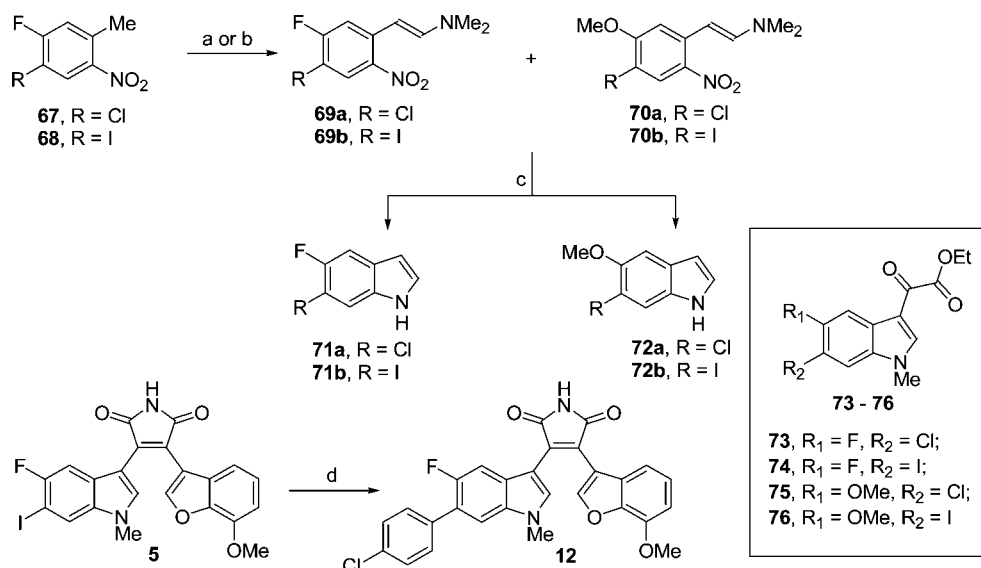
[a] Reagents and conditions: (a) DMF-DMA, 125 °C; (b) DMF-DIPA, 125 °C; (c) Fe, AcOH, EtOH; (d) Pd(PPh$_3$)$_4$, 4-chlorophenylboronic acid, K$_2$CO$_3$, DME/H$_2$O, 85 °C.

Table 2. CDK-2/CyclinE Inhibition by Substituted Maleimides[a]

compd	IC$_{50}$ (nM) CDK-2/cyclinE	IC$_{50}$ ratio CDK-2/cyclinE GSK-3β
staurosporine	3.8	0.8
1	1410	40
2	237	670
7	11700	12300
11	99000	410
14	1160	150
15	337	660
19	1840	2.6
21	1070	30
24	32000	130
31	149	27
32	27	5
33	3880	32300

[a] These compounds were tested at Reaction Biology, Inc. (http://www.reactionbiology.com).

compounds. Thus, almost all of the 5,6 and 5,7 disubstituted indoles (compounds **6**, **8**−**11**, and **20**) were found to be less potent than their monosubstituted analogs. The same effect occurred with 5-methoxy-substituted indolylmaleimides. The introduction of either Cl or I in the 6-position resulted in a ca. 2 (compound **28**) or 3.5 (compound **27**) fold decrease in activity relative to the case of the monosubstituted 5-methoxyindolyl-maleimide (IC$_{50}$ 125 nM).[18] It should be noted that an even more significant drop in activity was observed for compound **12** (IC$_{50}$ > 7 μM), which contains a larger *p*-chlorophenyl substituent in the 6-position. The SAR of the benzofuran component is as follows: the hydroxymethyl group attached to position 6 dramatically improved the potency of this scaffold; thus, the 6-hydroxymethylbenzofuranyl analogues **2**, **7**, and **15** were found to be the most potent among all 6-substituted benzofuranylmaleimides. This improvement is especially remarkable in the polysubstituted series, as can be seen by comparing maleimides **6** and **7**. Also, the maleimide **2** was 10-fold more potent than its 6-hydroxysubstituted analogue **4**. In contrast, the potency was significantly lower for compounds having methoxy (compound **8**, IC$_{50}$ 870 nM), cyclopropyl-methoxy (compound **9**, IC$_{50}$ > 1 μM), or cyclobutylmethoxy (compound **10**, IC$_{50}$ > 4 μM) attachments. Another observation related to the size and nature of the benzofuran counterpart

substitution is that the incorporation of side chains with terminal double (compound **17**, IC$_{50}$ 48.3 nM) or triple bonds (compound **16**, IC$_{50}$ 25.3 nM) generated compounds with comparable activities, while the *p*-methoxybenzyl derivative **18** turned out to be ca. 10-fold less potent. Compound **34**, with methoxymethyl and hydroxymethyl groups attached to the indole and benzofuran rings, respectively, that was synthesized to further improve the potency of the maleimide-containing scaffold, showed an IC$_{50}$ value at 0.73 ± 0.10 nM. It was even slightly less potent than **33** (IC$_{50}$ = 0.23 ± 0.04 nM).

In addition, the hydroxymethyl substituent at the 6-position of the benzofuran moiety provided an enhanced selectivity against CDK-2, as can be seen upon comparing the pairs of compounds **15** and **14** or **7** and **11** (Table 2). By contrast, the same group attached to the 7-position of the indolyl counterpart caused a considerable drop in selectivity (compounds **31** and **32**).

To ascertain whether molecular modeling could possibly explain the observed SAR results, compounds **2** and **31** were docked into the ATP binding site of GSK-3β (1R0E) (Figure 1).[25] Their binding poses were governed largely by two adjacent intermolecular hydrogen bonds: the NH group of the maleimide ring forms a hydrogen bond with the backbone carbonyl oxygen of Asp133, and one of the carbonyl oxygen atoms of the maleimide forms a hydrogen bond with the backbone NH of Val135. In addition to these main interactions, the 7-hydroxym-ethyl group of compound **31** appears to be within hydrogen bonding distance of the side chain of Arg141 (IC$_{50}$ = 5.4 nM), whereas the 6-hydroxymethyl group of compound **2** is within hydrogen bonding distance of the side chains of Gln185, Asn186, and Asp200 (IC$_{50}$ = 0.35 nM). In the case of compound **33**, having a 7-methoxymethyl group at the 7-position of the indole ring, its IC$_{50}$ of 0.23 nM was better than that found for **31**. While both the hydroxymethyl and methoxymethyl groups at the 7-position of the indole ring are able to H-bond with the nearby Arg residue, it is only the methoxymethyl group (as in **33**) that can help drive the inhibitor into its binding site, whereas the hydroxymethyl group of **31** may be less favorably oriented, as it points into the open area where it is accessible to solvent molecules. The modeling studies will find more solid ground
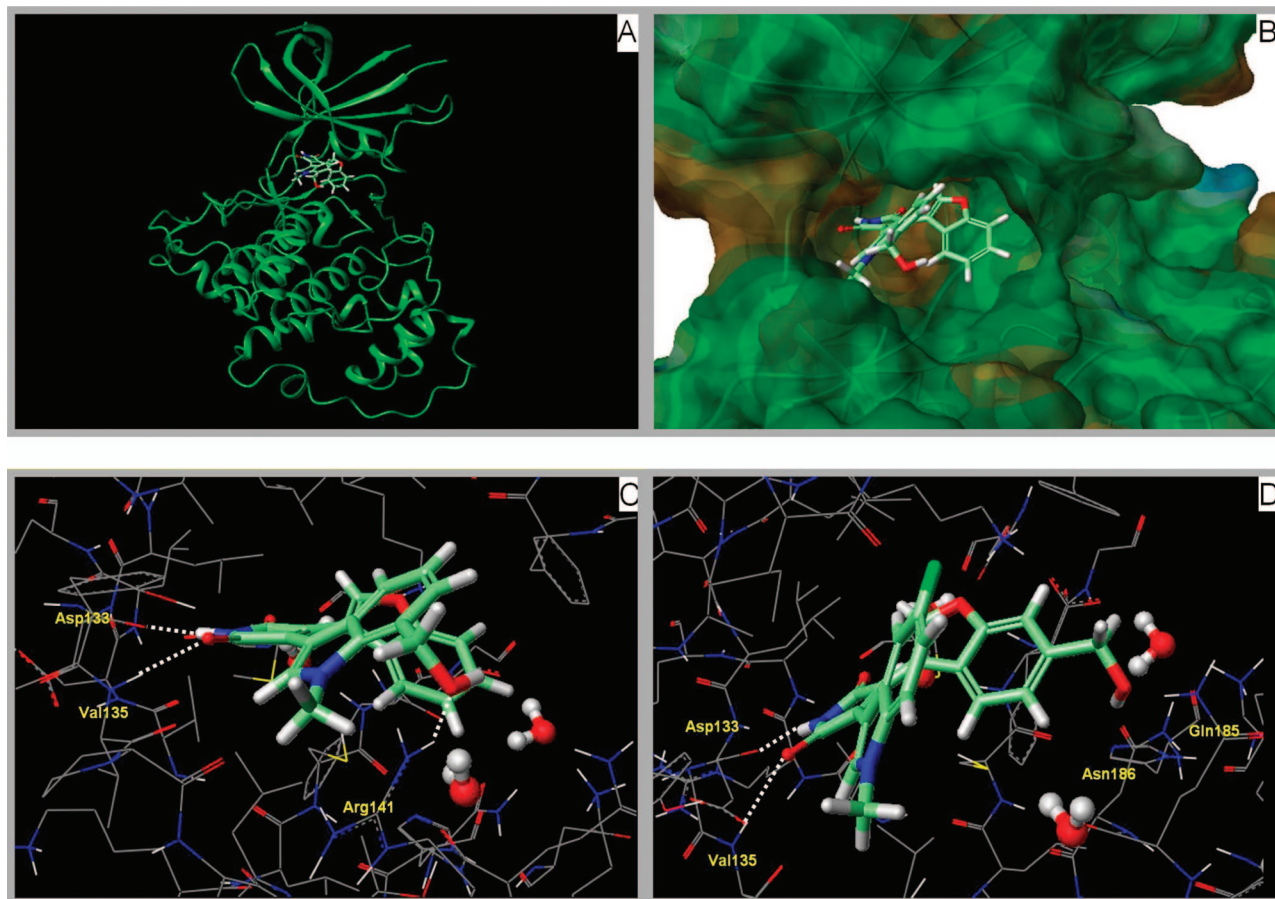
Figure 1. (A, B) Views of compound **31** docked into the GSK-3β binding site in which the backbone is shown as ribbons (A) and the protein surface is colored by lipophilic potential (blue = hydrophilic, brown = lipophilic) (B). (C) Docked pose of compound **31** in the GSK-3β binding site. The 7-hydroxymethyl group is within the hydrogen bonding distance of the Arg141 side chain. (D) Docked pose of compound **2** in the GSK-3β binding site. The 6-hydroxymethyl group is within hydrogen bonding distance of the Gln185 and Asn186 side chains.

once we complete X-ray cocrystal structures of some of these inhibitors bound to human GSK-3β.

GSK-3 Inhibitors Decrease Proliferation and Survival of Pancreatic Cancer Cells. A select few of the GSK-3β inhibitors that have different structural features and demonstrate varying potencies in the in vitro assay were examined for their capacity to decrease pancreatic cancer cell proliferation and survival. It was shown earlier that treatment of BXPC3, HupT3, and MiaPaCa-2 cells with the known GSK-3β inhibitors **77** and **78**, which we used as reference compounds, led to a significant decrease in pancreatic cancer cell proliferation.[16] Some of our new compounds, such as **5**, **6**, **11**, **20**, and **26**, showed activity similar to the reference compounds but exhibited better efficacy (Table 3).

The two most potent compounds, **5** and **26**, and the inactive compound **27** (Table 3) were tested for their ability to inhibit GSK-3β in cell lines. Using Western immunoblotting, we estimated GSK-3β activity by monitoring the level of phosphorylation of glycogen synthase (GS), a substrate of GSK-3β. The two most potent compounds, **5** and **26**, effectively inhibited GSK-3β activity, as shown by a decrease in GS phosphorylation (Figure 2A) leading to decreased proliferation and survival of BXPC3 and HupT3 pancreatic cancer cells (Table 3; Figure 2A, B, D). Compound **27**, however, did not affect GSK-3β activity, proliferation, or survival of pancreatic cancer cells (Table 3; Figure 2B, C). Consistent with the idea that GSK-3β positively regulates NFκB-mediated pancreatic cancer cell survival,[16] we found that treatment with the GSK-3β inhibitors

Table 3. Growth Inhibition of Pancreatic Cancer Cells by Selected Maleimides

	IC$_{50}$ (μM) $\pm$ SD		
compd	MiaPaCa-2[a]	BXPC3[a]	HupT3[a]
77	29.0 $\pm$ 1.7	14.0 $\pm$ 0.6	22.0 $\pm$ 2.1
78	25.0 $\pm$ 0.9	NT[b]	NT[b]
5	0.6 $\pm$ 0.1	0.9 $\pm$ 0.2	0.6 $\pm$ 0.1
6	3.0 $\pm$ 0.4	2.0 $\pm$ 0.2	2.0 $\pm$ 0.3
7	7 $\pm$ 1	5.0 $\pm$ 0.7	2.1 $\pm$ 1.5
11	3.0 $\pm$ 0.2	1.0 $\pm$ 0.2	1.0 $\pm$ 0.1
13	30.0 $\pm$ 2.2	NT[b]	43.0 $\pm$ 6.3
20	2.0 $\pm$ 0.2	0.9 $\pm$ 0.1	2.0 $\pm$ 0.1
21	8.0 $\pm$ 0.6	33 $\pm$ 4	>50
22	28.0 $\pm$ 4.1	42.0 $\pm$ 7.6	42.0 $\pm$ 8.3
25	34.0 $\pm$ 2.2	>50	>50
26	5.0 $\pm$ 0.9	1.0 $\pm$ 0.2	0.6 $\pm$ 0.1
27	>50	>50	>50
30	8.0 $\pm$ 1.2	6.0 $\pm$ 0.8	6.0 $\pm$ 0.5
33	>50	>50	27.0 $\pm$ 4.2
38	17.0 $\pm$ 3.2	7.0 $\pm$ 2.1	6.0 $\pm$ 0.7

[a] The pancreatic cancer cell lines MiaPaCa-2, BXPC3, and HupT3 were obtained from ATCC (Rockville, MD). MTS assay was carried out according to the manufacturer protocol. 72 h post-treatment, cell viability was measured and compounds' IC$_{50}$ values were determined [b] Not tested.

5 and **26** resulted in a pronounced decrease in NFκB-mediated expression of XIAP, the most potent antiapoptotic protein, leading to subsequent apoptosis in pancreatic cancer cells (Figure 2A, B, D). Again, compound **27** had no such effect (Figure 2B, C) even at concentrations up to 50 μM (Table 3). As expected, compound **5** showed significant anticancer activity at concentrations of 1−5 μM (Table 3). In addition, compound
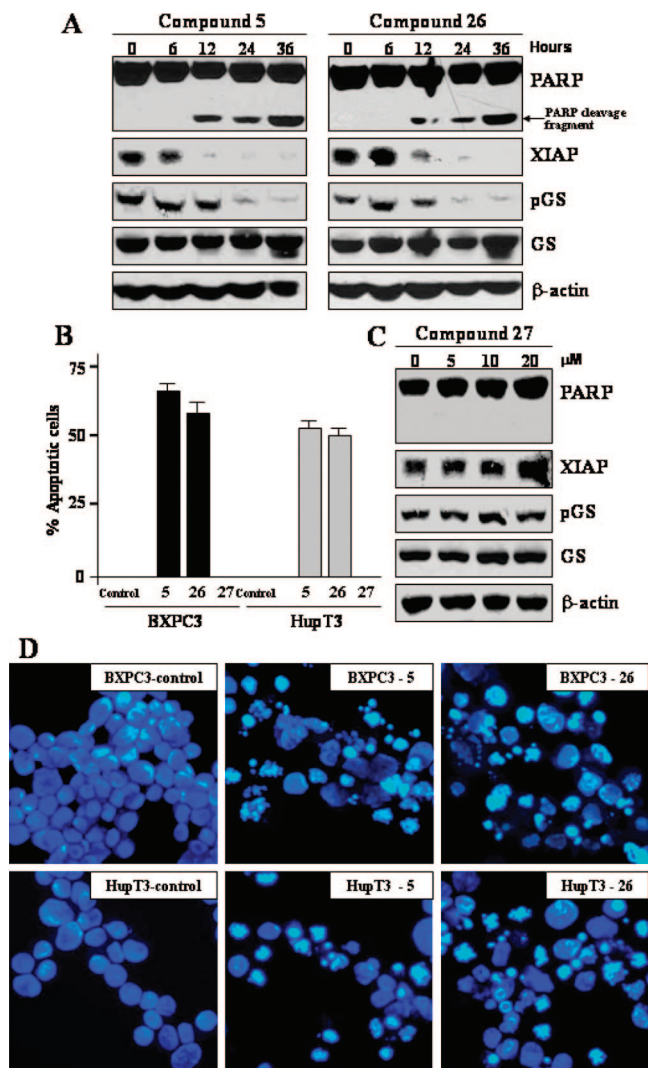
Figure 2. Treatment with GSK-3β inhibitors induces apoptosis in pancreatic cancer cells. (A) BXPC3 pancreatic cancer cells were treated with GSK-3β inhibitors **5** (5 μM) and **26** (5 μM) for 6, 12, 24, and 36 h, as indicated. Whole cell lysates were prepared, separated by SDS-PAGE (50 μg/well), transferred to a PVDF membrane, and probed with indicated antibodies. pGS, phosphorylated glycogen synthase; GS, glycogen synthase. (B) BXPC3 and HupT3 pancreatic cancer cells were treated with **5** (5 μM), **26** (5 μM), or **27** (20 μM) for 36 h. The percentage of apoptotic cells was determined by Hoechst staining as previously described.[26] Columns, mean; bars, SD; control, DMSO; **5**; **26**; **27**. (C) BXPC3 pancreatic cancer cells were treated with different concentrations of **27** which included 5, 10, and 20 μM. At 36 h post-treatment, whole cell lysates were prepared and analyzed as in part A. (D) Representative Hoechst staining pictures of BXPC3 and HupT3 pancreatic cancer cells treated with compounds **5** (5 μM) and **26** (5 μM) for 36 h.

5 was evaluated against a panel of kinases and found to be selective (Table 2 in the Supporting Information).

Our results demonstrated that although some of these compounds are potent GSK-3β inhibitors, as shown by the in vitro kinase assay, they did not inhibit GSK-3β activity in cell culture and, therefore, showed no anticancer effect in pancreatic cancer cells. The discrepancy regarding the effect in the in vitro kinase assay compared to the cell culture experiments is not surprising. Chemoresistance is intrinsic to cancer. The common reason for resistance to a broad range of drugs is overexpression of permeability-glycoprotein (P-gp) and other drug transporters (ATP-binding cassette) that detect and eject anticancer drugs from cancer cells. This could result in failure to achieve effective

intracellular concentrations for some compounds that are lipophilic and should show excellent ability to cross biological membrane. In summary, because the maleimides **13**, **21**, **22**, **25**, **27**, and **33** (Table 3) showed little or no inhibitory activity in the cell proliferation studies, it is possible that these compounds are being recognized and ejected by energy-dependent transporters or detoxified by a CYP-mediated mechanism in the pancreatic cancer cells, a point worthy of further investigation.

Conclusion

A library of benzofuran-3-yl-(indol-3-yl)maleimides was designed, synthesized, and tested for their selectivity and potency as GSK-3β inhibitors relative to other homologous kinases. Selected compounds were examined in turn for their ability to suppress pancreatic cancer cell proliferation and survival in vitro. We have been able to show that some of these compounds, namely compounds **5**, **6**, **11**, **20**, and **26**, demonstrate good antiproliferative activity against a panel of pancreatic cancer cell lines, which consisted of MiaPaCa-2, BXPC3, and HupT3. Most notable was our finding that the treatment of BXPC3 with inhibitors **5** and **26** resulted in a distinct decrease in NFκB-mediated expression of XIAP, the most potent antiapoptotic protein, leading to subsequent apoptosis in these pancreatic cancer cells. Because of these valuable results, we plan to prepare a wider variety of GSK-3β inhibitors implementing modifications aimed at improving compound druggability (aqueous solubility and metabolic stability) through both substitutent modifications and alteration in the scaffold in order to arrive at possible clinical candidates for pancreatic cancer therapy.

Experimental Section

Synthesis of Benzofuran-3-yl-(indol-3-yl)maleimides. ^{1}H NMR and ^{13}C NMR spectra were recorded on a Bruker spectrometer at 400 and 100 MHz, respectively, with TMS as an internal standard. Standard abbreviations indicating multiplicity were used as follows: s = singlet, bs = broad singlet, d = doublet, t = triplet, q = quadruplet, and m = multiplet. HRMS experiments were performed on LTO-FTICR or Shimadzu IT-TOF mass spectrometers. TLC was performed with Merck 250-mm 60F$_{254}$ silica gel plates. Preparative TLC was performed with Analtech 1000-mm silica gel GF plates. Column chromatography was performed using Merck silica gel (40−60 mesh). Analytical HPLC was carried out on an Ace 3AQ column (100 mm × 4.6 mm), with a Shimadzu 10 VP Series HPLC with a diode array detector; flow rate = 2.0 mL/min; from 10% acetonitrile in water to 50% in 10 min and to 100% acetonitrile in 5 min with 0.05% TFA (method A) or from 30% acetonitrile in water to 100% of acetonitrile in 15 min with 0.05% TFA (method B) or from 30% acetonitrile in water to 100% of acetonitrile in 30 min with 0.05% TFA (method C); a column Ace AQ5 (250 mm × 10 mm) was used with this last method. The purity of key target compounds determined by HPLC (methods A, B, or C) was higher than 95% (Table 3 in the Supporting Information).

Compounds **1**, **13**, **19**, **24**, **29**, and **37** were described in our previous publication.[18]

General Procedures for the Preparation of Maleimides. The following methods represent the typical procedures for the synthesis of the benzofuranylindolylmaleimide-based compounds.

Synthesis of the Indole Moiety. To a solution of substituted indole (1 equiv) in dry DMF (2 mL/mmol) cooled with an ice bath was added NaH (55% suspension in mineral oil, 1.5 equiv), followed by MeI (1.2 equiv), after which the reaction mixture was allowed to warm to room temperature. The reaction was monitored by TLC. After completion, the reaction mixture was poured into ice−water and the solution was extracted with EtOAc. The organic

phase was washed with water and brine, dried over anhydrous Na$_2$SO$_4$, and concentrated in vacuo. The crude was purified by column chromatography (from hexane to EtOAc−hexane; 1:3) or filtered through silica gel (EtOAc−hexane; 1:3) and subjected to further reaction without additional purification. To a solution of substituted 1-methyl-1H-indole in Et$_2$O (5 mL/mmol) cooled to 0 °C was added ethyl oxalyl chloride (6 equiv) dropwise. The reaction mixture was stirred for 0.5 h at 0 °C, allowed to warm to room temperature, and stirred until completion. The reaction was quenched by addition of water, and the reaction mixture was diluted with EtOAc. The organic layer was washed with saturated NaHCO$_3$, water, and brine and was dried over anhydrous Na$_2$SO$_4$ and concentrated. The residue was purified by column chromatography (EtOAc−hexane; 1:3) to give the substituted (1-methyl-1H-indol-3-yl)oxo-acetic acid ethyl ester.

Formation of the Benzofuran Counterpart. Benzofuran-3-ylacetic Acid Ethyl Esters. To a solution of substituted or unsubstituted benzofuran-3-one (1 equiv) in toluene (35 mL/mmol) was added (carbethoxymethylene)triphenylphosphorane (4 equiv), and the mixture was refluxed overnight or until completion. When needed, an additional amount (1 or 2 equiv) of (carbethoxymethylene)triphenylphosphorane was added and the mixture was refluxed until completion. The reaction mixture was cooled to room temperature and concentrated. The residue was purified by column chromatography (hexane to ethyl acetate−hexane; 1:3) to give the product.

2-Benzofuran-3-ylacetamides. Product obtained from the previous step was added to liquid ammonia at −78 °C, and the reaction flask was sealed and heated at 50−60 °C until completion. The reaction mixture was cooled to −78 °C and allowed to reach room temperature slowly so that the excess of ammonia was evaporated, and residue was washed with hexane to afford the substituted or unsubstituted 2-benzofuran-3-ylacetamide, which was used without further purification.

Benzofuran-3-yl-(indol-3-yl)maleimides. To a suspension of substituted or unsubstituted 2-benzofuran-3-ylacetamide (1 equiv) and substituted or unsubstituted indolyl-3-glyoxylate (1 equiv) in dry THF (10 mL/mmol) at 0 °C, a 1.0 M solution of tert-BuOK in THF (4 equiv) was added dropwise, and the reaction mixture was stirred at room temperature for several hours until completion. The reaction mixture was quenched with water and diluted with EtOAc. The organic phase was washed with brine and then dried over Na$_2$SO$_4$ and evaporated in vacuo. When deprotection of the silyl ether was required, the residue was dissolved in THF (20 mL/mmol) and a 1.0 M solution of TBAF in THF (1.5 equiv) was added at room temperature. The mixture was stirred for 2 h. The reaction mixture was quenched with NH$_4$Cl and stirred for 5 min. The solvent was removed, and the residue was dissolved in CH$_2$Cl$_2$ and washed twice with water and brine. The organic phase was dried over Na$_2$SO$_4$ and concentrated. The residue was purified by preparative TLC (EtOAc−hexane, 1:1, or MeOH−CH$_2$Cl$_2$, 5:95) or column chromatography (EtOAc−hexane, 1:9 to 1:1, or MeOH−CH$_2$Cl$_2$, 1:99 to 1:9) to afford product. The yields were in the range 20−72%.

3-(5-Fluoro-1-methyl-1H-indol-3-yl)-4-(6-hydroxymethylbenzofuran-3-yl)pyrrole-2,5-dione (2). ^{1}H NMR (DMSO-d_6, 400 MHz) δ 3.88 (s, 3H), 4.52 (d, J = 5.7 Hz, 2H), 5.24 (t, J = 5.7 Hz, 1H), 6.53 (dd, J = 2.3, 10.3 Hz, 1H), 6.84 (d, J = 8.1 Hz, 1H), 6.89 (d, J = 8.2 Hz, 1H), 6.95 (dt, J = 2.4, 9.1 Hz, 1H), 7.49 (dd, J = 4.5, 9.5 Hz, 1H), 7.54 (s, 1H), 8.02 (s,1H), 8.24 (s,1H), 11.19 (s,1H); ^{13}C NMR (DMSO-d_6, 100 MHz) 33.7, 63.1, 104.27, 104.31, 103.1, 106.3, 109.4, 110.5, 110.8, 111.7, 112.2, 112.3, 121.5, 121.9, 122.9, 124.5, 126.4, 126.5, 132.6, 133.9, 136.2, 140.6, 147.4, 154.9, 156.5, 172.2, 172.5; FAB-HRMS calcd for C$_{22}$H$_{15}$FN$_2$O$_4$ [M + H]$^+$: 391.1089; found: 391.1089, calcd for C$_{22}$H$_{15}$FN$_2$O$_4$ [M + Na]$^+$: 413.0908; found: 413.0907.

3-(5-Fluoro-1-methyl-1H-indol-3-yl)-4-(6-methoxymethylbenzofuran-3-yl)pyrrole-2,5-dione (3). ^{1}H NMR (CDCl$_3$, 400 MHz) δ 3.33 (s, 3H), 3.86 (s, 3H), 4.48 (s, 2H), 6.64 (dd, J = 2.2, 9.8 Hz, 1H), 6.81−6.90 (m, 3H), 7.21 (dd, J = 4.5, 8.9 Hz, 1H), 7.39 (brs, 1H), 7.49 (s,1H), 7.79 (s,1H), 8.12 (s,1H); FAB-HRMS calcd

for C$_{23}$H$_{17}$FN$_2$O$_4$ [M + H]$^+$: 405.1245; found: 405.1243, calcd for C$_{22}$H$_{15}$FN$_2$O$_4$ [M + Na]$^+$: 427.1065; found: 427.1061.

3-(5-Fluoro-1-methyl-1H-indol-3-yl)-4-(6-hydroxybenzofuran-3-yl)pyrrole-2,5-dione (4). ^{1}H NMR (DMSO-d_6, 400 MHz) δ 3.88 (s, 3H), 6.39 (dd, J = 2.0, 8.5 Hz, 1H), 6.54 (dd, J = 2.2, 10.5 Hz, 1H), 6.61 (d, J = 8.5 Hz, 1H), 6.92 (d, J = 1.8 Hz, 1H), 6.95 (dt, J = 2.0, 8.5 Hz, 1H), 7.49 (dd, J = 4.5, 9.0 Hz, 1H), 7.98 (s, 1H), 8.09 (s, 1H), 9.58 (s, 1H), 11.16 (s, 1H); FAB-HRMS calcd for C$_{21}$H$_{13}$N$_2$O$_4$F [M − H]$^-$: 375.0781; found: 375.0773. (Partially degraded after few weeks at room temperature).

3-(5-Fluoro-6-iodo-1-methyl-1H-indol-3-yl)-4-(7-methoxybenzofuran-3-yl)pyrrole-2,5-dione (5). ^{1}H NMR (CDCl$_3$, 400 MHz,) δ 3.83 (s, 3H), 4.02 (s, 3H), 6.42 (d, J = 7.9 Hz, 1H), 6.73 (d, J = 7.5 Hz, 1H), 6.76 (d, J = 9.0 Hz, 1H), 6.83 (t, J = 7.9 Hz, 1H), 7.67 (m, 2H), 7.73 (s, 1H), 8.16 (s, 1H); FAB-HRMS calcd for C$_{22}$H$_{14}$N$_2$O$_4$FI [M + Na]$^+$: 538.9875; found: 538.9866.

3-Benzofuran-3-yl-4-(6-chloro-5-fluoro-1-methyl-1H-indol-3-yl)pyrrole-2,5-dione (6). ^{1}H NMR (CDCl$_3$, 400 MHz) δ 3.81 (s, 3H), 6.75−6.80 (m, 2H), 6.87 (t, J = 4.7 Hz, 1H), 7.20 (t, J = 4.5 Hz, 1H), 7.31 (m, 2H), 7.50 (d, J = 5.0 Hz, 1H), 7.73 (s, 1H), 8.14 (s, 1H); FAB-HRMS calcd for C$_{21}$H$_{12}$N$_2$O$_3$ClF [M + H]$^+$: 395.0599; found: 395.0617.

3-(6-Chloro-5-fluoro-1-methyl-1H-indol-3-yl)-4-(6-hydroxymethylbenzofuran-3-yl)pyrrole-2,5-dione (7). ^{1}H NMR (CDCl$_3$, 400 MHz) δ 3.83 (s, 3H), 4.67 (s, 2H), 6.75 (d, J = 10 Hz, 1H), 6.77 (d, J = 8.0 Hz, 1H), 6.87 (d, J = 8.0 Hz, 1H), 7.33 (d, J = 6.0 Hz, 1H), 7.52 (s, 1H), 7.77 (s, 1H), 8.14 (s, 1H); FAB-HRMS calcd for C$_{22}$H$_{14}$N$_2$O$_4$FCl [M + H]$^+$: 425.0699; found: 425.0713.

3-(6-Chloro-5-methoxy-1-methyl-1H-indol-3-yl)-4-(6-methoxybenzofuran-3-yl)pyrrole-2,5-dione (8). ^{1}H NMR (CD$_3$CN, 400 MHz) δ 4.33 (s, 3H), 4.39 (s, 3H), 7.07 (dd, J = 1.2, 5.2 Hz, 1H), 7.21 (d, J = 5.2 Hz, 1H), 7.34 (d, J = 6.5 Hz, 1H), 7.67 (d, J = 1.2 Hz, 1H), 8.12 (d, J = 3.7 Hz, 1H), 8.37 (s, 1H), 8.64 (s, 1H), 9.25 (s, 1H); FAB-HRMS calcd for C$_{22}$H$_{14}$N$_2$O$_4$ClF [M − H]$^-$: 423.0553; found: 423.0559.

3-(6-Chloro-5-methoxy-1-methyl-1H-indol-3-yl)-4-(6-cyclopropylmethoxybenzofuran-3-yl)pyrrole-2,5-dione (9). ^{1}H NMR (CD$_3$CN, 400 MHz) δ 0.32 (m, 2H), 0.60 (m, 2H), 1.21 (m, 1H), 3.80 (d, J = 7.0 Hz, 2H), 3.84 (s, 3H), 6.48 (dd, J = 2.2, 8.7 Hz, 1H), 6.63 (d, J = 8.7 Hz, 1H), 6.70 (d, J = 10.5 Hz, 1H), 7.07 (d, J = 2.0 Hz, 1H), 7.56 (d, J = 6.3 Hz, 1H), 7.82 (s, 1H), 8.08 (s, 1H), 8.70 (s, 1H); FAB-HRMS calcd for C$_{25}$H$_{18}$N$_2$O$_4$ClF [M + H]$^+$: 465.1012; found: 465.1010.

3-(6-Chloro-5-methoxy-1-methyl-1H-indol-3-yl)-4-(6-cyclobutylmethoxybenzofuran-3-yl)pyrrole-2,5-dione (10). ^{1}H NMR (CD$_3$CN, 400 MHz) δ 1.84−1.88 (m, 4H), 1.95−1.99 (m, 2H), 2.75 (m, 1H), 3.83 (s, 3H), 3.93 (d, J = 7.1 Hz, 2H), 6.47 (dd, J = 2.1, 8.8 Hz, 1H), 6.62 (d, J = 8.8 Hz, 1H), 6.77 (d, J = 10.6 Hz, 1H), 7.08 (d, J = 2.1 Hz, 1H), 7.54 (d, J = 7.3 Hz, 1H), 7.81 (s, 1H), 7.81 (s, 1H), 8.08 (s, 1H), 8.7 (s, 1H); FAB-HRMS calcd for C$_{26}$H$_{20}$N$_2$O$_4$ClF [M − H]$^-$: 477.1023; found: 477.1024.

3-(6-Chloro-5-fluoro-1-methyl-1H-indol-3-yl)-4-(7-methoxybenzofuran-3-yl)pyrrole-2,5-dione (11). ^{1}H NMR (CDCl$_3$, 400 MHz) δ 3.82 (s, 3H), 4.00 (s, 3H), 6.38 (d, J = 7.7 Hz, 1H), 6.71 (d, J = 7.5 Hz, 1H), 6.80 (m, 2H), 7.31 (d, 1H), 7.52 (s, 1H), 7.74 (s, 1H), 8.16 (s, 1H); FAB-HRMS calcd for C$_{22}$H$_{14}$N$_2$O$_4$ClF [M − H]$^-$: 423.0553; found: 423.0557.

3-[6-(4-Chlorophenyl)-5-fluoro-1-methyl-1H-indol-3-yl]-4-(7-methoxybenzofuran-3-yl)pyrrole-2,5-dione (12). 3-(5-Fluoro-6-iodo-1-methyl-1H-indol-3-yl)-4-(7-methoxybenzofuran-3-yl)pyrrole-2,5-dione (5) (0.020 g, 0.039 mmol), Pd(PPh$_3$)$_4$ (4.5 mg, 0.004 mmol), and 4-chlorophenylboronic acid (15.1 mg, 0.097 mmol) were dissolved in dimethoxyethane (DME) (4 mL), and the mixture was degassed for 1 min and stirred for 10 min at room temperature. A 2 M K$_2$CO$_3$ solution (2 M, 0.049 mL, 0.098 mmol) was added. The mixture was degassed again for 1 min and stirred at 85 °C overnight. The resulting mixture was cooled to ambient temperature and poured into a mixture of 0.1 N HCl/EtOAc (15 mL/15 mL). After partitioning, the organic layer was washed with water, filtered, and concentrated. The residue was purified by preparative TLC using (EtOAc−hexane, 1:1) to afford 12 as an orange solid (10

mg, 51%). The sample was further purified by HPLC for biological testing. ^{1}H NMR (CDCl$_3$, 400 MHz,) δ 3.89 (s, 3 H), 4.02 (s, 3 H), 6.53 (d, 1 H, J = 7.8 Hz), 6.74 (d, 1 H, J = 7.8 Hz), 6.90−6.82 (m, 2 H), 7.26 (m, 1 H), 7.48−7.39 (m, 4 H), 7.53 (s, 1 H), 7.79 (s, 1 H), 8.15 (s, 1H); FAB-HRMS calcd for C$_{28}$H$_{18}$N$_2$O$_4$FCl [M + Na]$^+$: 523.0832; found: 523.0824.

3-(5-Bromo-1-methyl-1H-indol-3-yl)-4-(7-methoxybenzofuran-3-yl)pyrrole-2,5-dione (14). ^{1}H NMR (CDCl$_3$, 400 MHz) δ 3.82 (s, 1H), 4.00 (s, 3H), 6.37 (d, J = 7.8 Hz, 1H), 6.71 (d, J = 7.8 Hz, 1H), 6.78 (t, J = 7.8 Hz, 1H), 7.14−7.23 (m, 3H), 7.37 (bs, 1H), 7.70 (3, 1H), 8.14 (s, 1H); FAB-HRMS calcd for C$_{22}$H$_{15}$N$_2$O$_4$Br [M + H]$^+$: 451.0293; found: 451.0279.

3-(5-Bromo-1-methyl-1H-indol-3-yl)-4-(6-hydroxymethylbenzofuran-3-yl)pyrrole-2,5-dione (15). ^{1}H NMR (DMSO-d_6, 400 MHz) δ 3.86 (s, 3H), 4.52 (d, J = 5.6 Hz, 2H), 5.26 (t, J = 6.0 Hz, 1H), 6.79 (d, J = 8.0 Hz, 1H), 6.89 (d, J = 8.0 Hz, 1H), 7.1 (d, J = 2.0 Hz, 1H), 7.21 (dd, J = 1.6, 8.8 Hz, 1H), 7.45 (d, J = 8.8 Hz, 1H), 7.55 (s, 1H), 7.96 (s, 1H), 8.26 (s, 1H), 11.20 (s, 1H); FAB-HRMS calcd for C$_{25}$H$_{18}$BrN$_2$O$_4$ [M + H]$^+$: 451.0288; found: 451.0288.

3-(5-Bromo-1-methyl-1H-indol-3-yl)-4-(6-prop-2-ynyloxybenzofuran-3-yl)pyrrole-2,5-dione (16). ^{1}H NMR (CDCl$_3$, 400 MHz) δ 3.83 (s, 3H), 4.67 (s, 1H), 5.42 (d, J = 3.9 Hz, 1H), 6.53−6.69 (m, 3H), 6.81 (t, J = 4.5 Hz, 1H), 7.22−7.12 (m, 6H), 7.71 (s, 1H), 8.08 (s, 1H); FAB-HRMS calcd for C$_{24}$H$_{15}$BrN$_2$O$_4$ [M + H]$^+$: 475.0288; found: 475.0297; calcd for C$_{24}$H$_{15}$BrN$_2$O$_4$ [M + Na]$^+$: 497.0108; found: 497.0119. (Partially degraded after a few weeks at room temperature).

3-(6-Allyloxybenzofuran-3-yl)-4-(5-bromo-1-methyl-1H-indol-3-yl)pyrrole-2,5-dione (17). ^{1}H NMR (DMSO-d_6, 400 MHz) δ 3.84 (s, 3H), 4.99 (s, 2H), 6.59 (dd, J = 1.8, 8.7 Hz, 1H), 6.69 (d, J = 8.7 Hz, 1H), 6.92 (d, J = 1.8 Hz, 1H), 7.20 (dd, J = 1.5, 8.5 Hz, 1H), 7.31−7.34 (m, 2H), 7.44 (d, J = 8.5 Hz, 1H), 7.94 (s, 1H), 8.17 (s, 1H), 11.20 (s, 1H); FAB-HRMS calcd for C$_{24}$H$_{17}$N$_2$O$_4$Br [M + H]$^+$: 477.0445; found: 477.0445.

3-(5-Bromo-1-methyl-1H-indol-3-yl)-4-[6-(4-methoxybenzyloxy)benzofuran-3-yl]pyrrole-2,5-dione (18). ^{1}H NMR (DMSO-d_6, 400 MHz) δ 3.75 (s, 3H), 3.84 (s, 3H), 4.99 (s, 2H), 6.61 (dd J = 2.0, 8.7 Hz, 1H), 6.70 (d, J = 8.7 Hz, 1H), 6.91 (d, J = 8.5 Hz, 1H), 7.04 (d, J = 1.5 Hz, 1H), 7.04 (dd, J = 1.5, 8.6 Hz, 1H), 7.31−7.36 (m, 3H), 7.45 (d, J = 8.6 Hz, 1H), 7.94 (1s, 1H), 8.17 (s, 1H); FAB-HRMS calcd for C$_{29}$H$_{21}$N$_2$O$_5$Br [M − H]$^−$: 579.0526; found: 579.0521.

3-(5,7-Dibromo-1-methyl-1H-indol-3-yl)-4-(7-methoxybenzofuran-3-yl)pyrrole-2,5-dione (20). ^{1}H NMR (CDCl$_3$, 400 MHz) δ 4.00 (s, 3H), 4.17 (s, 3H), 6.30 (d, J = 7.8 Hz, 1H), 6.73 (d, J = 7.8 Hz, 1H), 6.82 (t, J = 7.8 Hz, 1H), 7.12 (d, J = 1.7 Hz, 1H), 7.37 (d, J = 1.7 Hz, 1H), 7.55 (s, 1H), 7.61 (s, 1H), 8.93 (s, 1H); FAB-HRMS calcd for C$_{22}$H$_{14}$N$_2$O$_4$Br$_2$ [M − H]$^−$: 526.9248; found: 526.9247.

3-Benzofuran-3-yl-4-(5-iodo-1-methyl-1H-indol-3-yl)pyrrole-2,5-dione (21). ^{1}H NMR (DMSO-d_6, 400 MHz) δ 3.87 (s, 3H), 6.88 (d, J = 7.8 Hz, 1H), 6.94 (t, J = 7.8 Hz, 1H), 7.14 (s, 1H), 7.25 (t, J = 8.0 Hz, 1H), 7.63 (d, J = 8.2 Hz, 1H), 7.95 (s, 1H), 8.26 (s, 1H), 11.20 (s, 1H); FAB-HRMS calcd for C$_{21}$H$_{13}$N$_2$O$_3$I [M + H]$^+$: 469.0044; found: 469.0045.

3-(5-Fluorobenzofuran-3-yl)-4-(5-iodo-1-methyl-1H-indol-3-yl)pyrrole-2,5-dione (22). ^{1}H NMR (DMSO-d_6, 400 MHz) δ 3.87 (s, 3H), 6.65 (dd, J = 2.5, 9.0 Hz, 1H), 7.12 (m, 1H), 7.39 (m, 2H), 7.68 (dd, J = 4.0, 9.0 Hz, 1H), 7.98 (s, 1H), 8.31 (s, 1H), 11.18 (s, 1H); FAB-HRMS calcd for C$_{21}$H$_{12}$N$_2$O$_3$FI [M − H]$^−$: 484.9804; found: 484.9815.

3-[4-(6-Hydroxymethylbenzofuran-3-yl)-2,5-dioxo-2,5-dihydro-1H-pyrrol-3-yl]-1-methyl-1H-indole-5-carbonitrile (23). ^{1}H NMR (DMSO-d_6, 400 MHz) δ 3.91 (s, 3H), 4.51 (d, J = 5.7 Hz, 2H), 5.25 (t, J = 5.8 Hz, 1H), 6.68 (d, J = 8.1 Hz, 1H), 6.85 (d, J = 8.2 Hz, 1H), 7.40 (s, 1H), 7.47 (dd, J = 1.2, 8.5 Hz, 1H), 7.55 (s, 1H), 7.68 (d, J = 8.6 Hz, 1H), 8.05 (s, 1H), 8.33 (s, 1H), 11.27 (s, 1H); FAB-HRMS calcd for C$_{23}$H$_{15}$N$_3$O$_4$ [M + Na]$^+$: 420.0955; found: 420.0952.

3-(5-Cyclopropylethynyl-1-methyl-1H-indol-3-yl)-4-(5-fluorobenzofuran-3-yl)pyrrole-2,5-dione (25). ^{1}H NMR (CDCl$_3$, 400 MHz) δ 0.67 (m, 2H), 0.82 (m, 2H), 1.34 (m, 1H), 3.87 (s, 3H), 6.59 (d, J = 8.7 Hz, 1H), 6.97−6.93 (m, 2H), 7.17 (d, J = 8.3 Hz, 1H), 7.22 (d, J = 8.4 Hz, 1H), 7.46−7.43 (m, 1H), 7.53 (br s, 1H), 7.81 (s, 1H), 8.10 (s, 1H); FAB-HRMS calcd for C$_{26}$H$_{16}$N$_2$O$_3$F [M − H]$^−$: 423.1150; found: 423.1147.

3-(5-Fluorobenzofuran-3-yl)-4-(5-methyl-5H-[1,3]dioxolo[4,5-f]indol-7-yl)pyrrole-2,5-dione (26). ^{1}H NMR (CDCl$_3$, 400 MHz) δ 3.79 (s, 3H), 5.80 (m, 2H), 6.29 (s, 1H), 6.59 (dd, J = 2.4, 9.0 Hz, 1H), 6.74 (s, 1H), 6.91 (td, J = 2.5, 9.0 Hz, 1H), 7.41 (dd, J = 4.1, 8.0 Hz, 1H), 7.65 (s, 1H), 7.95 (s, 1H), 8.13 (s, 1H); FAB-HRMS calcd for C$_{22}$H$_{13}$N$_2$O$_5$F [M + H]$^+$: 405.0881; found: 405.0880.

3-Benzofuran-3-yl-4-(6-chloro-5-methoxy-1-methyl-1H-indol-3-yl)pyrrole-2,5-dione (27). ^{1}H NMR (DMSO-d_6, 400 MHz) δ 3.11 (s, 3H), 3.83 (s, 3H), 6.30 (s, 1H), 6.93 (t, J = 4.7 Hz, 1H), 7.04 (d, J = 4.7 Hz, 1H), 7.22 (t, J = 5.2 Hz, 1H), 7.30 (d, J = 1.7 Hz, 1H), 7.47 (d, J = 5.2 Hz, 1H), 7.86 (s, 1H), 8.01 (s, 1H); FAB-HRMS calcd for C$_{22}$H$_{15}$N$_2$O$_4$Cl [M + H]$^+$: 407.0793; found: 407.0793.

3-Benzofuran-3-yl-4-(6-iodo-5-methoxy-1-methyl-1H-indol-3-yl)pyrrole-2,5-dione (28). ^{1}H NMR (CDCl$_3$, 400 MHz) δ 3.09 (s, 3H), 3.83 (s, 3H), 6.29 (s, 1H), 6.96 (t, J = 4.7 Hz, 1H), 7.08 (d, J = 4.7 Hz, 1H), 7.21 (m, 2H), 7.47 (m, 2H), 7.69 (s, 1H), 7.86 (s, 1H), 8.00 (s, 1H); FAB-HRMS calcd for C$_{22}$H$_{15}$N$_2$O$_4$I [M + H]$^+$: 441.0149; found: 441.0149.

3-(7-Methoxybenzofuran-3-yl)-4-(1-methyl-6-trifluoromethyl-1H-indol-3-yl)pyrrole-2,5-dione (30). ^{1}H NMR (CDCl$_3$, 400 MHz) δ 3.94 (s, 3H), 4.02 (s, 3H), 6.43 (d, J = 7.8 Hz, 1H), 6.71 (d, J = 8.0 Hz, 1H), 6.81 (t, J = 8.0 Hz, 1H), 7.12 (m, 2H), 7.62 (s, 1H), 7.70 (s, 1H), 7.88 (s, 1H), 8.14 (s, 1H); FAB-HRMS calcd for C$_{23}$H$_{15}$N$_2$O$_4$F$_3$ [M + H]$^+$: 441.1062; found: 441.1057.

3-Benzofuran-3-yl-4-(7-hydroxymethyl-1-methyl-1H-indol-3-yl)pyrrole-2,5-dione (31). ^{1}H NMR (CDCl$_3$, 400 MHz) δ 1.77 (t, J = 6.0 Hz, 1H), 4.22 (s, 3H), 4.98 (d, J = 6.0 Hz, 2H), 6.72 (t, J = 7.6 Hz, 1H), 6.86−6.95 (m, 2H), 6.98 (t, J = 7.2 Hz, 2H), 7.19 (dt, J = 1.4, 7.5 Hz, 1H), 7.47 (t, J = 8.3 Hz, 1H), 7.56 (br s, 1H), 7.72 (s, 1H), 8.09 (s, 1H); FAB-HRMS calcd for C$_{22}$H$_{16}$N$_2$O$_4$ [M − H]$^−$: 371.1037; found: 371.1038.

3-(6-Hydroxymethylbenzofuran-3-yl)-4-(7-hydroxymethyl-1-methyl-1H-indol-3-yl)pyrrole-2,5-dione (32). ^{1}H NMR (DMSO-d_6, 400 MHz) δ 4.18 (s, 3H), 4.52 (d, J = 5.6 Hz, 2H), 4.84 (d, J = 5.6 Hz, 2H), 5.25 (t, J = 6.0 Hz, 1H), 5.36 (t, J = 6.0 Hz, 1H), 6.66 (t, J = 7.2 Hz, 1H), 6.80 (d, J = 8.0 Hz, 1H), 6.90 (s, 2H), 6.97 (d, J = 6.8 Hz, 1H), 7.51 (s, 1H), 7.89 (s, 1H), 8.18 (s, 1H), 11.18 (s, 1H); FAB-HRMS calcd for C$_{23}$H$_{18}$N$_2$O$_5$ [M + H]$^+$: 403.1289; found: 403.1287; calcd for C$_{23}$H$_{18}$N$_2$O$_5$ [M + Na]$^+$: 425.1107; found: 425.1107.

3-Benzofuran-3-yl-4-(7-methoxymethyl-1-methyl-1H-indol-3-yl)pyrrole-2,5-dione (33). ^{1}H NMR (DMSO-d_6, 400 MHz) δ 3.26 (s, 3H), 4.10 (s, 3H), 4.73 (s, 2H), 6.63 (t, J = 7.6 Hz, 1H), 6.83 (d, J = 7.6 Hz, 1H), 6.86−6.93 (m, 2H), 6.96 (d, J = 7.2 Hz, 1H), 7.20 (dt, J = 1.4, 7.2 Hz, 1H), 7.57 (d, J = 8.4 Hz, 1H), 7.88 (s, 1H), 8.25 (s, 1H), 11.19 (br s, 1H); FAB-HRMS calcd for C$_{23}$H$_{18}$N$_2$O$_4$ [M + H]$^+$: 387.1339; found: 387.1342; calcd for C$_{23}$H$_{18}$N$_2$O$_4$ [M + Na]$^+$: 409.1159; found: 409.1161.

3-(6-Hydroxymethylbenzofuran-3-yl)-4-(7-methoxymethyl-1-methyl-1H-indol-3-yl)pyrrole-2,5-dione (34). ^{1}H NMR (DMSO-d_6, 400 MHz) δ 3.27 (s, 3H), 4.11 (s, 3H), 4.50 (d, J = 8.0 Hz, 2H), 4.73 (s, 2H), 5.23 (t, J = 8.0 Hz, 1H), 6.66 (t, J = 7.6 Hz, 1H), 6.80−6.89 (m, 3H), 6.97 (d, J = 7.6 Hz, 1H), 7.50 (s, 1H), 7.88 (s, 1H), 8.21 (s, 1H), 11.19 (br s, 1H); FAB-HRMS calcd for C$_{24}$H$_{20}$N$_2$O$_5$ [M − H]$^−$: 415.1294; found: 415.1297.

3-[3-(4-Benzofuran-3-yl-2,5-dioxo-2,5-dihydro-1H-pyrrol-3-yl)-1-methyl-1H-indol-7-yl]propionic Acid Ethyl Ester (35). To a solution of 3-[3-(4-benzofuran-3-yl-2,5-dioxo-2,5-dihydro-1H-pyrrol-3-yl)-1-methyl-1H-indol-7-yl]acrylic acid ethyl ester (**68**) (45 mg, 0.10 mmol) in (MeOH−THF, 3:1) (20 mL) was added successively at 0 °C NiCl$_2$·6H$_2$O (24 mg, 0.10 mmol) and NaBH$_4$ (7.7 mg, 0.20 mmol), and the mixture was stirred at this temperature

for 15 min and then at room temperature for 2 h. The resulting mixture was diluted with EtOAc and washed with saturated aqueous NaHCO$_3$ solution. The aqueous phase was extracted with EtOAc, and the combined organic phases were dried over Na$_2$SO$_4$ and evaporated in vacuo. The residue was purified by preparative TLC (EtOAc−hexane; 4:6) followed by a purification by HPLC with method C to yield the product (20 mg, 45%). ^{1}H NMR (CDCl$_3$, 400 MHz) δ 1.25 (t, $J = 7.2$ Hz, 3H), 2.67 (t, $J = 8.2$ Hz, 2H), 3.40 (t, $J = 8.2$ Hz, 2H), 4.08−4.18 (m, 5H), 6.68 (t, $J = 7.6$ Hz, 1H), 6.81−6.93 (m, 4H), 7.18 (dt, $J = 1.5$, 7.4 Hz, 3H), 7.45 (d, $J = 8.3$ Hz, 1H), 7.66 (s, 1H), 7.79 (s, 1H), 8.08 (s, 1H); FAB-HRMS calcd for C$_{26}$H$_{22}$N$_2$O$_5$ [M + H]$^+$: 443.1602; found: 443.1613.

3-[3-(4-Benzofuran-3-yl-2,5-dioxo-2,5-dihydro-1H-pyrrol-3-yl)-1-methyl-1H-indol-7-yl]propionic Acid (36). The 3-[3-(4-benzofuran-3-yl-2,5-dioxo-2,5-dihydro-1H-pyrrol-3-yl)-1-methyl-1H-indol-7-yl]propionic acid ethyl ester (**35**) (8 mg, 0.018 mmol) was dissolved in EtOH (2 mL), and 1 N NaOH (0.072 mL, 0.072 mmol) was added to the solution. The mixture was stirred at room temperature overnight. The solvent was evaporated in vacuo, and water and 1 N HCl were added to reach pH 2. The acidic solution was extracted with EtOAc three times. The combined organic layers were washed with water and brine, dried over Na$_2$SO$_4$, and evaporated. The residue was first purified by preparative TLC (MeOH−CH$_2$Cl$_2$; 1:9) followed by a purification by HPLC with method C to yield the product (3 mg, 39%). ^{1}H NMR (CD$_3$OD, 400 MHz) δ 2.66 (t, $J = 7.8$ Hz, 2H), 3.40 (t, $J = 7.8$ Hz, 2H), 4.15 (s, 3H), 6.60 (t, $J = 7.8$ Hz, 1H), 6.61−6.82 (m, 3H), 6.87 (d, $J = 7.0$ Hz, 3H), 7.15 (m, 1H), 7.45 (d, $J = 8.3$ Hz, 3H), 7.73 (s, 1H), 8.13 (s, 1H); FAB-HRMS calcd for C$_{24}$H$_{18}$N$_2$O$_5$ [M + H]$^+$: 415.1289; found: 415.1304.

3-(5,6-Difluorobenzofuran-3-yl)-4-(1-methyl-1H-benzo[g]indol-3-yl)pyrrole-2,5-dione (38). ^{1}H NMR (CDCl$_3$, 400 MHz) δ 4.41 (s, 3H), 6.66 (dd, $J = 7.8$, 10.2 Hz, 1H), 6.96 (d, $J = 8.7$ Hz, 1H), 7.18 (d, $J = 8.7$ Hz, 1H), 7.27 (m, 2H), 7.44 (t, $J = 7.8$ Hz, 1H), 7.56 (t, $J = 7.0$ Hz, 1H), 7.70 (s, 1H), 7.82 (d, $J = 7.8$ Hz, 1H), 8.17 (s, 1H), 8.47 (d, $J = 8.4$ Hz, 1H); FAB-HRMS calcd for C$_{25}$H$_{14}$N$_2$O$_3$F$_2$ [M + H]$^+$: 429.1050; found: 429.1059.

GSK-3β in Vitro Kinase Assay. The in vitro kinase assay was performed in a 40 μL reaction volume containing 250 ng GSK-3β Calbiochem (EMD Biosciences, La Jolla, CA), 10 μM pGS peptide (RRRPASVPPSPSLSRHSS(P)HQRR, where the priming phosphoserine is underlined), 10 μM γ^{32}P ATP and increasing concentrations of the inhibitors in kinase buffer (20 mM MOPS pH 7.2, 15 mM MgCl$_2$, 5 mM EGTA, 25 mM β-glycerol phosphate, 1 mM Na$_3$VO$_4$, 1 mM DTT). The inhibitors were allowed to bind GSK-3β for 10 min prior to the addition of peptide. The reaction was started by the addition of the ATP solution and was carried out at 30 °C for 30 min, after which 25 μL of the reaction mixture was spotted on P81 Whatman filters (Florham Park, NJ), dried, washed twice with 0.75% H$_3$PO$_4$, and rinsed with acetone. The dried filters were placed in scintillation vials containing 2 mL of Scinti-safe Econo 2 solution (Fisher Scientific, Pittsburgh, PA) and read in a Beckman Coulter LS 600IC (Fullerton, CA) scintillation counter.

IC$_{50}$ Determination. The data were plotted as average percent activity versus the log of the concentration of inhibitor. The IC$_{50}$ was determined according to NIH guidelines (http://www.ncgc. nih.gov/guidance/section3.html) and the 4-parameter logistic plot (4PL), which calculates the relative IC$_{50}$ based on the maximum (top) and minimum (bottom) percent activities as well as the Hill slope. In some cases, the 4PL did not give an accurate fitting of the data (error fit above 40%), and thus, a 3-parameter logistic fit top (3PLFT) or a 3-parameter logistic fit bottom (3PLFB) was used to obtain the IC$_{50}$ using the equation $y = $ bottom $ + $ (top $-$ bottom)/ $(1 + 10((\log \text{IC}_{50} - x)\text{HillSlope}))$ from Graphpad Prism 5. This program displays the log IC$_{50}$ as well as the IC$_{50}$ and gives the standard error of the log IC$_{50}$, which was converted back to the percent fitting error of the IC$_{50}$ by using the equation %FE(IC$_{50}$) = FE(log IC$_{50}$) ln(10) $\times$ 100.

Cytotoxicity Assay. Materials and Methods. Immunoblot Analysis and Antibodies. For immunoblots, cells were lysed as described previously.[15] Protein sample concentration was quantified, and an equal amount (50 μg of whole protein extract) of protein was loaded in each well of SDS-polyacrylamide (PAGE) gel. Cell or tissue extracts were separated by 10% SDS-PAGE, transferred to polyvinylidene difluoride membrane (PVDF), and probed as indicated. Antibodies for immunoblot analysis were obtained from the following suppliers: PARP and XIAP from BD Biosciences Pharmingen (San Diego, CA); phospho-glycogen synthase (Ser641) and glycogen synthase from Cell Signaling Technologies (Beverly, MA); β-actin from Novus (Littleton, CO). Bound antibodies were detected as previously described.

MTS Assay. A 3-(4,5-dimethylthiazol-2-yl)-5-(3-carboxymethoxyphenyl)-2-(4-sulfophenyl)-2H-tetrazolium assay from Promega (Madison, WI) was carried out in the presence or absence of the potential GSK-3 inhibitors according to the manufacturer's protocol. 72 h post-treatment, cell viability was measured and compounds' IC$_{50}$ values were determined.

Supporting Information Available: Molecular modeling methods, experimental procedures for some intermediates, ^{13}C NMR data, HPLC purity data for all final compounds, and selectivity data for compounds **5**, **7**, **11**, **15**, and **33**. These materials are available free of charge via the Internet at http://pubs.acs.org.

References

(1) Embi, N.; Rylatt, D. B.; Cohen, P. Glycogen synthase kinase-3 from rabbit skeletal muscle. Separation from cyclic-AMP-dependent protein kinase and phosphorylase kinase. *Eur. J. Biochem./FEBS* **1980**, *107*, 519–527.

(2) Woodgett, J. R. Molecular cloning and expression of glycogen synthase kinase-3/factor A. *EMBO J.* **1990**, *9*, 2431–2438.

(3) Cohen, P.; Goedert, M. GSK3 inhibitors: development and therapeutic potential. *Nat. Rev. Drug Discovery* **2004**, *3*, 479–487.

(4) Kim, L.; Kimmel, A. R. GSK3, a master switch regulating cell-fate specification and tumorigenesis. *Curr. Opin. Genet. Dev.* **2000**, *10*, 508–514.

(5) Hamelers, I. H.; van Schaik, R. F.; Sipkema, J.; Sussenbach, J. S.; Steenbergh, P. H. Insulin-like growth factor I triggers nuclear accumulation of cyclin D1 in MCF-7S breast cancer cells. *J. Biol. Chem.* **2002**, *277*, 47645–47652.

(6) Thiel, A.; Heinonen, M.; Rintahaka, J.; Hallikainen, T.; Hemmes, A.; Dixon, D. A.; Haglund, C.; Ristimèaki, A. Expression of cyclooxygenase-2 is regulated by glycogen synthase kinase-3beta in gastric cancer cells. *J. Biol. Chem.* **2006**, *281*, 4564–4569.

(7) Gregory, M. A.; Qi, Y.; Hann, S. R. Phosphorylation by glycogen synthase kinase-3 controls c-myc proteolysis and subnuclear localization. *J. Biol. Chem.* **2003**, *278*, 51606–51612.

(8) Cohen, Y.; Chetrit, A.; Cohen, Y.; Sirota, P.; Modan, B. Cancer morbidity in psychiatric patients: influence of lithium carbonate treatment. *Med. Oncol.* **1998**, *15*, 32–36.

(9) Johnson, C. D.; Puntis, M.; Davidson, N.; Todd, S.; Bryce, R. Randomized, dose-finding phase III study of lithium gamolenate in patients with advanced pancreatic adenocarcinoma. *Br. J. Surg.* **2001**, *88*, 662–668.

(10) Ring, D. B.; Johnson, K. W.; Henriksen, E. J.; Nuss, J. M.; Goff, D. Selective glycogen synthase kinase 3 inhibitors potentiate insulin activation of glucose transport and utilization in vitro and in vivo. *Diabetes* **2003**, *52*, 588–595.

(11) Yuan, H.; Mao, J.; Li, L.; Wu, D. Suppression of glycogen synthase kinase activity is not sufficient for leukemia enhancer factor-1 activation. *J. Biol. Chem.* **1999**, *274*, 30419–30423.

(12) Shakoori, A.; Ougolkov, A.; Yu, Z. W.; Zhang, B.; Modarressi, M. H.; Mai, M.; Takahashi, Y.; Minamoto, T. Deregulated GSK3beta activity in colorectal cancer: its association with tumor cell survival and proliferation. *Biochem. Biophys. Res. Commun.* **2005**, *334*, 1365–1373.

(13) Mai, W.; Miyashita, K.; Shakoori, A.; Zhang, B.; Yu, Z. W.; Takahashi, Y.; Motoo, Y.; Kawakami, K.; Minamoto, T. Detection of active fraction of glycogen synthase kinase 3beta in cancer cells by nonradioisotopic in vitro kinase assay. *Oncology* **2006**, *71*, 297–305.

(14) Buss, H.; Dèorrie, A.; Schmitz, M. L.; Frank, R.; Livingstone, M.; Resch, K.; Kracht, M. Phosphorylation of serine 468 by GSK-3beta negatively regulates basal p65 NF-kappaB activity. *J. Biol. Chem.* **2004**, *279*, 49571–49574.

(15) Ougolkov, A. V.; Fernandez-Zapico, M. E.; Savoy, D. N.; Urrutia, R. A.; Billadeau, D. D. Glycogen synthase kinase-3beta participates in nuclear factor kappaB-mediated gene transcription and cell survival in pancreatic cancer cells. *Cancer Res.* **2005**, *65*, 2076–2081.

(16) Ougolkov, A. V.; Bone, N. D.; Fernandez-Zapico, M. E.; Kay, N. E.; Billadeau, D. D. Inhibition of glycogen synthase kinase-3 activity leads to epigenetic silencing of nuclear factor kappaB target genes and induction of apoptosis in chronic lymphocytic leukemia B cells. *Blood* **2007**, *110*, 735–742.

(17) Meijer, L.; Flajolet, M.; Greengard, P. Pharmacological inhibitors of glycogen synthase kinase 3. *Trends Pharmacol. Sci.* **2004**, *25*, 471–480.

(18) Kozikowski, A. P.; Gaisina, I. N.; Yuan, H.; Petukhov, P. A.; Blond, S. Y.; Fedolak, A.; Caldarone, B.; McGonigle, P. Structure-based design leads to the identification of lithium mimetics that block mania-like effects in rodents. Possible new GSK-3beta therapies for bipolar disorders. *J. Am. Chem. Soc.* **2007**, *129*, 8328–8332.

(19) Bentley, J. M.; Adams, D. R.; Bebbington, D.; Benwell, K. R.; Bickerdike, M. J.; Davidson, J. E.; Dawson, C. E.; Dourish, C. T.; Duncton, M. A.; Gaur, S.; George, A. R.; Giles, P. R.; Hamlyn, R. J.; Kennett, G. A.; Knight, A. R.; Malcolm, C. S.; Mansell, H. L.; Misra, A.; Monck, N. J.; Pratt, R. M.; Quirk, K.; Roffey, J. R.; Vickers, S. P.; Cliffe, I. A. Indoline derivatives as 5-HT(2C) receptor agonists. *Bioorg. Med. Chem. Lett.* **2004**, *14*, 2367–2370.

(20) Bentley, J. M.; Davidson, J. E.; Duncton, M. A. J.; Giles, P. R.; Pratt, R. M. Use of a Modified Leimgruber-Batcho Reaction to Prepare 6-Chloro-5-fluoroindole. *Synth. Commun.* **2004**, *34*, 2295–2300.

(21) Ponticello, G. S.; Baldwin, J. J. Useful Synthesis of 4-Substituted Indoles. *J. Org. Chem.* **1979**, *44*, 4003–4005.

(22) Bhat, R.; Xue, Y.; Berg, S.; Hellberg, S.; Ormèo, M.; Nilsson, Y.; Radesèater, A. C.; Jerning, E.; Markgren, P. O.; Borgegêard, T.; Nylèof, M.; Gimâenez-Cassina, A.; Hernâandez, F.; Lucas, J. J.; Dâiaz-Nido, J.; Avila, J. Structural insights and biological effects of glycogen synthase kinase 3-specific inhibitor AR-A014418. *J. Biol. Chem.* **2003**, *278*, 45937–45945.

(23) Smith, D. G.; Buffet, M.; Fenwick, A. E.; Haigh, D.; Ife, R. J.; Saunders, M.; Slingsby, B. P.; Stacey, R.; Ward, R. W. 3-Anilino-4-arylmaleimides: potent and selective inhibitors of glycogen synthase kinase-3 (GSK-3). *Bioorg. Med. Chem. Lett.* **2001**, *11*, 635–639.

(24) Vulpetti, A.; Crivori, P.; Cameron, A.; Bertrand, J.; Brasca, M. G.; D'Alessio, R.; Pevarello, P. Structure-based approaches to improve selectivity: CDK2-GSK3beta binding site analysis. *J. Chem. Inf. Model.* **2005**, *45*, 1282–1290.

(25) Kim, K. H.; Gaisina, I.; Gallier, F.; Holzle, D.; Blond, S. Y.; Mesecar, A.; Kozikowski, A. P. Use of Molecular Modelling, Docking, and 3D-QSAR Studies for the Determination of the Binding Mode of 3-Benzofuranyl-4-indolyl-maleimides as GSK-3β Inhibitors. *J. Mol. Model.* **2009**, in press.

(26) Armstrong, D. K.; Kaufmann, S. H.; Ottaviano, Y. L.; Furuya, Y.; Buckley, J. A.; Isaacs, J. T.; Davidson, N. E. Epidermal growth factor-mediated apoptosis of MDA-MB-468 human breast cancer cells. *Cancer Res.* **1994**, *54*, 5280–5283.